Diffusional Aspects for the Chlorination of the Sulfonated Poly(styrene-co-Divinylbenzene) Resin Beads

SON-KI IHM* and JOU-HYEON AHN, *Department of Chemical Engineering, Korea Advanced Institute of Science and Technology, P.O. Box 131, Cheongryang, Seoul, Korea,* HARTMUT WIDDECKE, KLAUS STRUß, and JOACHIM KLEIN, *Institut für Technische Chemie, Technische Universität Braunschweig, D-3300 Braunschweig, Germany*

Synopsis

The diffusional process in the chlorination of sulfonated poly(styrene-co-divinylbenzene) bead was investigated through a general model as well as direct observation with electron microprobe. Two modes of diffusion, namely the pore diffusion and gelular permeation, were analyzed by two system parameters through a two-phase model. The effective pore and gelular diffusivities estimated from the x-ray energy-dispersive analysis data on the chlorine profile and the conversion suggest that, even for the same crosslinking, the diffusivity of chlorine in the gelular bead is larger by several orders of magnitude than that for the gelular microparticle in the macroreticular bead.

INTRODUCTION

The most widely used polymer supports are the styrene-divinylbenzene copolymers composed of long-chain polystyrene crosslinked by divinylbenzene.[1] In view of the structural differences, the resins can be divided into two groups, gel and macroreticular resins.[2] Gelular resins have three-dimensional and homogeneous structure with no discontinuities, show no porosity in the dried state, and are accessible only by swelling. On the other hand, macroreticular resins have heterogeneous structure, consisting of the agglomerates of very small gelular microparticles, and have an inner surface even in the dried state. The macropores, the free space between the agglomerates, are accessible without swelling.[3,4] While gelular resins can function effectively only in a swelling medium, macroreticular resins are effective in both swelling and nonswelling solvents.

When these styrene-divinylbenzene copolymers, gelular and macroreticular, are functionalized, the permeation in the gelular phase plays an important part.[5] In many cases, the detailed knowledge of the distribution of functional groups throughout the polymer bead is very important because the

*To whom all correspondence should be addressed.

Journal of Applied Polymer Science, Vol. 37, 109–125 (1989)

CCC 0021-8995/89/010109-17$04.00

activity/selectivity and thermal stability of resin catalysts are usually influenced by the distribution of the functional groups.[6] However, until now there has been no sufficient analysis on the kinetics of the functionalization of the resins.

The aim of this article is to present a general model on the functionalization of both gelular and macroreticular resin beads such as the sulfonation of polymer beads or the chlorination[7,8] of the sulfonated polymer beads which is attempted to increase their catalytic activity and/or thermal stability. Direct observations on the chlorine profile will provide the necessary data for the estimation of the effective diffusivity.

EXPERIMENTAL

Samples

Ion-exchange resin beads with 8% crosslinking, which were sulfonated, were provided by Bayer A.G., and both gelular (SC 108) and macroreticular resins (SPC 108) were tested. Appropriate amounts of dry resins were immersed in the sulfuric acid solution for about 24 h until complete swelling was achieved.

Chlorination

A 1000 mL 4-neck flask was filled with 98% sulfuric acid solution and stirred by the magnetic bar, and the solution was saturated with the chlorine by flowing the gas continuously through the distributor. The chlorination started when a vial of the resin beads immersed in the sulfuric acid was poured into the flask. At a planned interval of time, some beads were sampled out and dried in the vacuum oven for further observations.

Direct Observation Through Electron Microprobe

The resin beads were cut flat through the center and their surfaces were coated by evaporating the graphite. The concentration profile of chlorine on the cut surface was observed by the X-ray energy-dispersive analysis (EDX). It should be understood that for a macroreticular bead the chlorine profile and the conversion are attributed solely to the gelular microparticles. The chlorine in the pore space was removed in the vacuum oven prior to the EDX observations. The conversion was calculated from the ratio of the intensity of the chlorine peak to that of the sulfur peak. Complete chlorination is assumed when the ratio is 0.9, and this value was used to normalize the conversion.

THEORY AND MATHEMATICAL DEVELOPMENT

Even though the chemical reaction is not necessarily faster than the various diffusional processes for some difficult reactions of resins, the theoretical development in this article is based on the assumption that the chemical reaction is much faster and not rate controlling. If the chemical reaction was rate controlling, the theoretical development would be rather straightforward.

Model for a Gelular Resin Bead

For the spherical gelular resin bead having a three-dimensional and homogeneous structure, the transient diffusion equation can be written as

$$\frac{\partial C_g}{\partial t} = \frac{D_g}{r_g^2}\frac{\partial}{\partial r_g}\left(r_g^2\frac{\partial C_g}{\partial r_g}\right) - \frac{\partial S_g}{\partial t} \tag{1}$$

where D_g is the permeability of reactants giving functional groups to the polymer bead and is assumed to be constant and S_g is the surface concentration of the reactants. And the necessary initial and boundary conditions are given as follows:

$$t=0; \quad C_g = 0 \quad \text{for} \quad 0 \le r_g \le R_g \tag{2a}$$

$$t>0; \quad C_g = C_g^0 \quad \text{for} \quad r_g = R_g \tag{2b}$$

$$\frac{\partial C_g}{\partial r_g} = 0 \quad \text{for} \quad r_g = 0 \tag{2c}$$

If the functionalization, a chemical reaction between the reactant and the monomer unit of the resin matrix, is very fast, the adsorption of the reactants can be assumed to be linear and irreversible, specifically:

$$S_g = K_g C_g$$

With the dimensionless variables defined as follows

$$\theta_g = \frac{C_g}{C_g^0}, \qquad \xi_g = \frac{r_g}{R_g}, \qquad \tau = \frac{D_g t}{R_g^2(1 + K_g)},$$

Eqs. (1) and (2) are rewritten in the dimensionless forms

$$\frac{\partial \theta_g}{\partial \tau} = \frac{1}{\xi_g^2}\frac{\partial}{\partial \xi_g}\left(\xi_g^2\frac{\partial \theta_g}{\partial \xi_g}\right) \tag{3}$$

$$\theta_g(0, \xi_g) = 0 \tag{4a}$$

$$\theta_g(\tau, 1) = 1 \tag{4b}$$

$$\frac{\partial \theta_g}{\partial \xi_g}(\tau, 0) = 0 \tag{4c}$$

The solution is easily found[9] to be

$$\theta_g = 1 + \frac{2}{\pi\xi_g}\sum_{n=1}^{\infty}\frac{(-1)^n}{n}e^{-n^2\pi^2\tau}\sin(n\pi\xi_g) \tag{5}$$

Removing the reactant that remains unreacted in the fluid phase, the total amount of functionalized reactants is given by

$$M_t = \int_o^{R_g} 4\pi r_g^2 S_g \, dr_g = 4\pi R_g^3 K_g C_g^0 \int_0^1 \xi_g^2 \theta_g \, d\xi_g.$$

At equilibrium,

$$M_\infty = \tfrac{4}{3}\pi R_g^3 K_g C_g^0$$

Therefore, the normalized amount of functionalized reactant is

$$\frac{M_t}{M_\infty} = 3\int_0^1 \xi_g^2 \theta_g \, d\xi_g \tag{6}$$

With θ_g given by Eq. (5), Eq. (6) becomes

$$\frac{M_t}{M_\infty} = 1 - \frac{6}{\pi^2} \sum_{n=1}^{\infty} \frac{1}{n^2} e^{-n^2\pi^2\tau} \tag{7}$$

Model for a Macroreticular Resin Bead

The macroreticular resin bead consists of many spherical microparticles with free space between them, which account for the porosity of the resin. Therefore, the macroreticular resin can be considered as two phases:[10] microspheres and pores formed by the space between the microspheres. The radii of microspheres are assumed to be uniform and much smaller than the bead size. The schematic diagram is shown in Figure 1. In reality, however, the morphology of microspheres is more complex and appears to consist of numerous nuclei. The exact analysis on this complex structure has yet to be made, but it is assumed in this present study that the microsphere has continuous gelular phase.

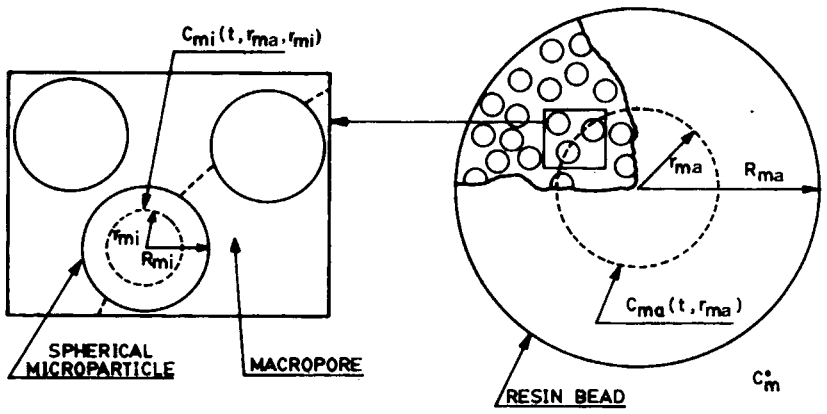

Fig. 1. Schematic diagram of a sulfonated poly(styrene-co-divinylbenzene) macroreticular resin bead.

Two different kinds of monomer units composing the polymer matrix exist in the microsphere of the macroreticular resin. The fraction γ of the total monomer units is located on the surface of the microsphere, providing easy access for the reactants. The functionalization of macroreticular resin can proceed with these external monomer units without being preceded by permeation into the microsphere. However, the remaining units of monomer units of the fraction $1 - \gamma$ are located within the microsphere. The reactants must therefore penetrate from the pore space into the microsphere in order to gain access to the inner monomer units.

According to the two-phase model, the governing equation can be written as follows:

For the pore space,

$$\frac{\epsilon D_{ma}}{r_{ma}^2}\frac{\partial}{\partial r_{ma}}\left(r_{ma}^2\frac{\partial C_{ma}}{\partial r_{ma}}\right) = \epsilon\frac{\partial C_{ma}}{\partial t} + \gamma\frac{\partial S_{ma}}{\partial t} + \frac{3(1-\epsilon)D_{mi}}{R_{mi}}\frac{\partial C_{mi}}{\partial r_{mi}}\bigg|_{r_{mi}=R_{mi}} \tag{8}$$

and for the microsphere,

$$\frac{D_{mi}}{r_{mi}^2}\frac{\partial}{\partial r_{mi}}\left(r_{mi}^2\frac{\partial C_{mi}}{\partial r_{mi}}\right) = \frac{\partial C_{mi}}{\partial t} + (1-\gamma)\frac{\partial S_{mi}}{\partial t} \tag{9}$$

where Eq. (8) implies that the diffusional flux is balanced by the accumulation due to the pore space, the disappearance due to reaction with the polymer matrix on the surface of the microsphere, and the permeation into the microspheres.

The necessary initial and boundary conditions are given as follows:

For the pore space,

$$t=0; \quad C_{ma} = 0 \quad \text{for} \quad 0 \le r_{ma} \le R_{ma} \tag{10a}$$

$$t>0; \quad C_{ma} = C_m^0 \quad \text{for} \quad r_{ma} = R_{ma} \tag{10b}$$

$$\frac{\partial C_{ma}}{\partial r_{ma}} = 0 \quad \text{for} \quad r_{ma} = 0 \tag{10c}$$

and for the microsphere

$$t=0; \quad C_{mi} = 0 \quad \text{for} \quad 0 \le r_{mi} \le R_{mi} \tag{11a}$$

$$t>0; \quad C_{mi} = C_{ma} \quad \text{for} \quad r_{mi} = R_{mi} \tag{11b}$$

$$\frac{\partial C_{mi}}{\partial r_{mi}} = 0 \quad \text{for} \quad r_{mi} = 0 \tag{11c}$$

where Eq. (11b) is valid only if the radius of the microsphere is much smaller than that of the polymer bead.

If the functionalization is very fast, the adsorption of the reactant can be assumed to be linear and irreversible, that is,

$$S_{ma} = K_{ma}C_{ma}$$

$$S_{mi} = K_{mi}C_{mi}$$

With the dimensionless variables and parameters defined as follows

$$\theta_{ma} = \frac{C_{ma}}{C_m^o} \qquad \theta_{mi} = \frac{C_{mi}}{C_m^o} \qquad \zeta = \frac{r_{ma}}{R_{ma}}$$

$$\xi = \frac{r_{mi}}{R_{mi}} \qquad \tau = \frac{D_{mi}t}{R_{mi}^2\{1 + (1 - \gamma)K_{mi}\}}$$

$$\alpha = \frac{D_{mi}/\{1 + (1 - \gamma)K_{mi}\}}{\epsilon D_{ma}/(\epsilon + \gamma K_{ma})} \times \frac{R_{ma}^2}{R_{mi}^2} = \frac{D'_{mi}/R_{mi}^2}{D'_{ma}/R_{ma}^2} = \frac{t_m}{t_i}$$

$$\beta = 3(1 - \epsilon)\frac{1 + (1 - \gamma)K_{mi}}{\epsilon + \gamma K_{ma}} \qquad \delta = \frac{\gamma K_{ma}}{\gamma K_{ma} + (1 - \gamma)K_{mi}}$$

Eqs. (8)–(11) can be rewritten in dimensionless form as follows

$$\frac{1}{\zeta^2}\frac{\partial}{\partial \zeta}\left(\zeta^2 \frac{\partial \theta_{ma}}{\partial \zeta}\right) = \alpha \frac{\partial \theta_{ma}}{\partial \tau} + \alpha\beta \frac{\partial \theta_{mi}}{\partial \xi}\bigg|_{\xi=1} \tag{12}$$

$$\frac{1}{\xi^2}\frac{\partial}{\partial \xi}\left(\xi^2 \frac{\partial \theta_{mi}}{\partial \xi}\right) = \frac{\partial \theta_{mi}}{\partial \tau} \tag{13}$$

$$\theta_{ma}(0, \zeta) = 0 \tag{14a}$$

$$\theta_{ma}(\tau, 1) = 1 \tag{14b}$$

$$\frac{\partial \theta_{ma}}{\partial \zeta}(\tau, 0) = 0 \tag{14c}$$

$$\theta_{mi}(0, \xi) = 0 \tag{15a}$$

$$\theta_{mi}(\tau, 1) = \theta_{ma} \tag{15b}$$

$$\frac{\partial \theta_{mi}}{\partial \xi}(\tau, 0) = 0 \tag{15c}$$

where the parameter α represents the ratio of t_m, the characteristic time required for diffusion through the pore space of resin bead and t_i, the characteristic time required for permeation through the microsphere and $\beta/3$ represents the ratio of the microsphere and pore space uptakes at equilibrium.

The analytic solutions of Eqs. (12) and (13) with Eqs. (14) and (15) are given by

$$\theta_{ma} = 1 + \frac{4\pi}{\alpha\beta\zeta} \sum_{k=1}^{\infty} \sum_{q=1}^{\infty} \frac{(-1)^k k \sin(k\pi\zeta) e^{-P_{qk}^2 \tau}}{P_{qk}^2 \{1 + 1/\beta + \cot^2 P_{qk} - (1 - k^2\pi^2/\alpha\beta) P_{qk}^2\}} \tag{16}$$

and

$$\theta_{mi} = \theta_{ma} + \frac{2}{\pi\xi} \sum_{m=1}^{\infty} \frac{(-1)^m}{m} \sin(m\pi\xi) e^{-m^2\pi^2\tau}$$

$$+ \frac{8}{\alpha\beta\zeta\xi} \sum_{m=1}^{\infty} \sum_{k=1}^{\infty} \sum_{q=1}^{\infty} \frac{k}{m}$$

$$\times \frac{(-1)^{m+k} \sin(k\pi\zeta) \sin(m\pi\xi) \left(P_{qk}^2 e^{-P_{qk}^2 \tau} - m^2\pi^2 e^{-m^2\pi^2\tau} \right)}{P_{qk}^2 \left(P_{qk}^2 - m^2\pi^2 \right) \{1 + 1/\beta + \cot^2 P_{qk} - (1 - k^2\pi^2/\alpha\beta)/P_{qk}^2\}} \tag{17}$$

where P_{qk} are the roots of the transcendental equation

$$\alpha P_{qk}^2 + \alpha\beta(1 - P_{qk} \cot P_{qk}) = k^2\pi^2, \qquad k = 1, 2, 3, \ldots \tag{18}$$

The Eq. (16) is equivalent to the form given by Ruckenstein et al.[11]

Removing the reactants that remain unreacted in the fluid phase, the concentration of the reactant attached to the polymer matrix is given by

$$S_m = \gamma S_{ma} + \frac{3(1 - \gamma)}{4\pi R_{mi}^3} \int_0^{R_{mi}} 4\pi r_{mi}^2 S_{mi} \, dr_{mi}$$

Therefore, the normalized concentration is given by

$$\theta_m = \frac{S_m / C_m^o}{\gamma K_{ma} + (1 - \gamma) K_{mi}} = \delta\theta_{ma} + 3(1 - \delta) \int_0^1 \xi^2 \theta_{mi} \, d\xi \tag{19}$$

where δ represents the ratio of the amount of reactant attached to the surface of microspheres to the total amount of reactants attached to polymer matrix and if K_{ma} and K_{mi} are the same, δ becomes γ. The total amount of the reactant attached to the polymer matrix is

$$M_t = \int_0^{R_{ma}} 4\pi r_{ma}^2 (1 - \epsilon) S_m \, dr_{ma}$$

The normalized amount of the reactant attached to the polymer matrix is also given by

$$\frac{M_t}{M_\infty} = 3 \int_0^1 \zeta^2 \theta_m \, d\zeta \tag{20}$$

Introducing Eqs. (16) and (17) into Eqs. (19) and (20) gives

$$\theta_m = 1 + \frac{4\delta\pi}{\alpha\beta\zeta}\sum_{k=1}^{\infty}\sum_{q=1}^{\infty}\frac{(-1)^k k\sin(k\pi\zeta)e^{-P_{qk}^2\tau}}{P_{qk}^2\left\{1 + 1/\beta + \cot^2 P_{qk} - \left(1 - k^2\pi^2/\alpha\beta\right)/P_{qk}^2\right\}}$$

$$- \frac{6(1-\delta)}{\pi^2}\sum_{m=1}^{\infty}\frac{1}{m^2}e^{-m^2\pi^2\tau}$$

$$+ \frac{24(1-\delta)\pi}{\alpha\beta\zeta}$$

$$\times \sum_{m=1}^{\infty}\sum_{k=1}^{\infty}\sum_{q=1}^{\infty}\frac{(-1)^k k\sin(k\pi\zeta)\left(e^{-m^2\pi^2\tau} - e^{-P_{qk}^2\tau}\right)}{P_{qk}^2\left(P_{qk}^2 - m^2\pi^2\right)\left\{1 + 1/\beta + \cot^2 P_{qk} - \left(1 - k^2\pi^2/\alpha\beta\right)/P_{qk}^2\right\}} \quad (21)$$

and

$$\frac{M_t}{M_\infty} = 1 - \frac{12\delta}{\alpha\beta}\sum_{k=1}^{\infty}\sum_{q=1}^{\infty}\frac{e^{-P_{qk}^2\tau}}{P_{qk}^2\left\{1 + 1/\beta + \cot^2 P_{qk} - \left(1 - k^2\pi^2/\alpha\beta\right)/P_{qk}^2\right\}}$$

$$- \frac{6(1-\delta)}{\pi^2}\sum_{m=1}^{\infty}\frac{1}{m^2}e^{-m^2\pi^2\tau}$$

$$- \frac{72(1-\delta)}{\alpha\beta}$$

$$\times \sum_{m=1}^{\infty}\sum_{k=1}^{\infty}\sum_{q=1}^{\infty}\frac{e^{-m^2\pi^2\tau} - e^{-P_{qk}^2\tau}}{P_{qk}^2\left(P_{qk}^2 - m^2\pi^2\right)\left\{1 + 1/\beta + \cot^2 P_{qk} - \left(1 - k^2\pi^2/\alpha\beta\right)/P_{qk}^2\right\}} \quad (22)$$

Results of Modeling Calculations

The parameter α is defined as the ratio of the time scales for the diffusional processes taking place in the pore space and the microparticle, respectively. Therefore, α gives a measure of the relative rates of the diffusion in the pore space and the permeation into the microparticle. For sufficiently large values of α, the pore diffusional process is rate determining while for very small values of α the microparticle permeation is rate determining.

The parameter β gives the information concerning the absorption capacity between the microparticle and the pore space at equilibrium. Therefore, for large values of β the capacity of the pore space is negligible while for very small values of β the microparticle capacity is negligible.

Functionalization with the microparticle permeation controlling. For very small values of α ($\alpha < 10^{-3}$), $t_m \ll t_i$, the rate of pore diffusion into the pore space is much faster than that of permeation into the microparticle so

that the pore space is essentially at equilibrium before some measurable permeation into the microparticle is observed. Thus, the diffusion into the pore space occurs first, followed by the microparticle permeation.

In this case, the transient diffusion equation and initial and boundary conditions can be written as follows:

For the pore space

$$\frac{\epsilon D_{ma}}{r_{ma}^2}\frac{\partial}{\partial r_{ma}}\left(r_{ma}^2\frac{\partial C_{ma}}{\partial r_{ma}}\right) = \epsilon\frac{\partial C_{ma}}{\partial t} + \gamma\frac{\partial S_{ma}}{\partial t} \tag{23}$$

$$C_{ma}(0, r_{ma}) = 0 \tag{24a}$$

$$C_{ma}(t, R_{ma}) = C_m^o \tag{24b}$$

$$\frac{\partial C_{ma}}{\partial r_{ma}}(t,0) = 0 \tag{24c}$$

and for the microparticle

$$\frac{D_{mi}}{r_{mi}^2}\frac{\partial}{\partial r_{mi}}\left(r_{mi}^2\frac{\partial C_{mi}}{\partial r_{mi}}\right) = \frac{\partial C_{mi}}{\partial t} + (1-\gamma)\frac{\partial S_{mi}}{\partial r_{mi}} \tag{25}$$

$$C_{mi}(0, r_{mi}) = 0 \tag{26a}$$

$$C_{mi}(t, R_{mi}) = C_m^o \tag{26b}$$

$$\frac{\partial C_{mi}}{\partial r_{mi}}(t,0) = 0 \tag{26c}$$

In terms of the aforementioned dimensionless variables and parameters, Eqs. (23)–(26) can be rewritten to give the analytic solutions

$$\theta_{ma} = 1 + \frac{2}{\pi\zeta}\sum_{n=1}^{\infty}\frac{(-1)^n}{n}\sin(n\pi\zeta)\exp(-n^2\pi^2\tau/\alpha) \tag{27}$$

and

$$\theta_{mi} = 1 + \frac{2}{\pi\xi}\sum_{n=1}^{\infty}\frac{(-1)^n}{n}\sin(n\pi\xi)\exp(-n^2\pi^2\tau) \tag{28}$$

Introducing Eqs. (27) and (28) into Eqs. (19) and (20), respectively, in order to obtain the functionalized quantity and concentration throughout the total polymer bead gives

$$\theta_m = 1 + \frac{2\delta}{\pi\zeta}\sum_{n=1}^{\infty}\frac{(-1)^n}{n}\sin(n\pi\zeta)\exp(-n^2\pi^2\tau/\alpha) - \frac{6(1-\delta)}{\pi^2}\sum_{n=1}^{\infty}\frac{1}{n^2}\exp(-n^2\pi^2\tau) \tag{29}$$

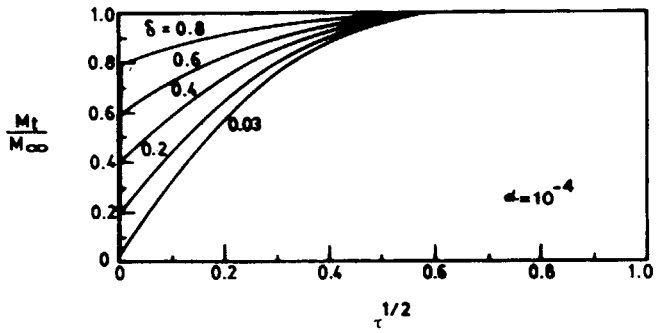

Fig. 2. Functionalization with the microparticle permeation controlling when $\alpha = 10^{-4}$.

and

$$\frac{M_t}{M_\infty} = 1 - \frac{6}{\pi^2}\left\{\delta \sum_{n=1}^{\infty} \frac{1}{n^2}\exp(-n^2\pi^2\tau/\alpha) + (1-\delta)\sum_{n=1}^{\infty}\frac{1}{n^2}\exp(-n^2\pi^2\tau)\right\} \tag{30}$$

Figure 2 shows the normalized amount of the functionalized reactant for the cases of $\delta = 0.03$ to $\delta = 0.8$ when $\alpha = 10^{-4}$. As shown in Figure 2, the two-step functionalization occurs. Since the pore diffusion rate is relatively much faster than the microparticle permeation rate, the quantity corresponding to γ, which is the fraction of the monomer units located on the surface of the microparticles of the total monomer units, is functionalized first very rapidly and a slow functionalization due to the microparticle permeation follows.

Functionalization with the pore diffusion controlling. For sufficiently large value of α ($\alpha > 100$), $t_m \gg t_i$, the microparticle permeation rate is relatively much faster than the pore diffusion rate. Therefore, the concentration in the microparticles may be considered to be uniform and the same as the corresponding local concentration in the pore space.

In this case, the material balance becomes as follows

$$\frac{\epsilon D_{ma}}{r_{ma}^2}\frac{\partial}{\partial r_{ma}}\left(r_{ma}^2\frac{\partial C_{ma}}{\partial r_{ma}}\right) = \epsilon\frac{\partial C_{ma}}{\partial t} + \gamma\frac{\partial S_{ma}}{\partial t} + (1-\epsilon)\left\{\frac{\partial C_{mi}}{\partial t} + (1-\gamma)\frac{\partial S_{mi}}{\partial t}\right\} \tag{31}$$

$$C_{mi}(t, r_{mi}) = C_{ma}(t, r_{ma}) \tag{32}$$

With the initial and boundary conditions of the Eq. (14), the solution of Eq. (31) is given by

$$\theta_{ma} = 1 + \frac{2}{\pi\zeta}\sum_{n=1}^{\infty}\frac{(-1)^n}{n}\sin(n\pi\zeta)\exp\left(-\frac{n^2\pi^2\tau}{\alpha + \alpha\beta/3}\right) \tag{33}$$

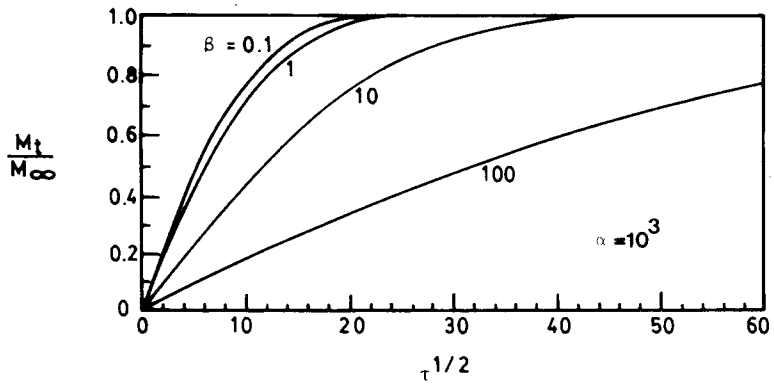

Fig. 3. Functionalization with the pore diffusion controlling when $\alpha = 10^3$.

and

$$\theta_{mi} = \theta_{ma} \tag{34}$$

The functionalized quantity and concentration profile throughout the polymer bead are given, respectively, by

$$\theta_m = 1 + \frac{2}{\pi\zeta}\sum_{n=1}^{\infty}\frac{(-1)^n}{n}\sin(n\pi\zeta)\exp\left(-\frac{n^2\pi^2\tau}{\alpha + \alpha\beta/3}\right) \tag{35}$$

and

$$\frac{M_t}{M_\infty} = 1 - \frac{6}{\pi^2}\sum_{n=1}^{\infty}\frac{1}{n^2}\exp\left(-\frac{n^2\pi^2\tau}{\alpha + \alpha\beta/3}\right) \tag{36}$$

The functionalized quantities for the case of $\alpha = 10^3$ are plotted with β varying from 0.1 to 100 in Figure 3. As the value of β increases, the rate of approach to complete conversion becomes slow. Since the microparticle permeation rate is very rapid, the microparticle existing near the surface of the polymer bead should be first saturated than that existing in the interior. Therefore, as β increases, the amount of reactants to diffuse into the interior of the polymer bead decreases and then the functionalization with the monomer units of interior polymer matrix becomes more difficult.

Functionalization with both pore diffusion and microparticle permeation controlling. For intermediate values of α ($10^{-3} < \alpha < 10^2$) the Eqs. (21) and (22) must be used.

Figure 4 shows the effect of α on the concentration profile throughout the macroreticular resin bead when $\beta = 1$. It can be shown that for the smaller value of α the concentrations are almost uniform throughout and the dimensionless time of approaching to equilibrium becomes shorter.

The functionalized quantities for the case of $\delta = 0.2$ and $\delta = 0.6$ are plotted in Figures 5 and 6 respectively, with varying α and β. These figures show that the smaller the values of α and β become, the faster the rate of approaching to equilibrium becomes. The effect of β is not important for small values of α. As the value of α increases, the effect of β becomes more important.

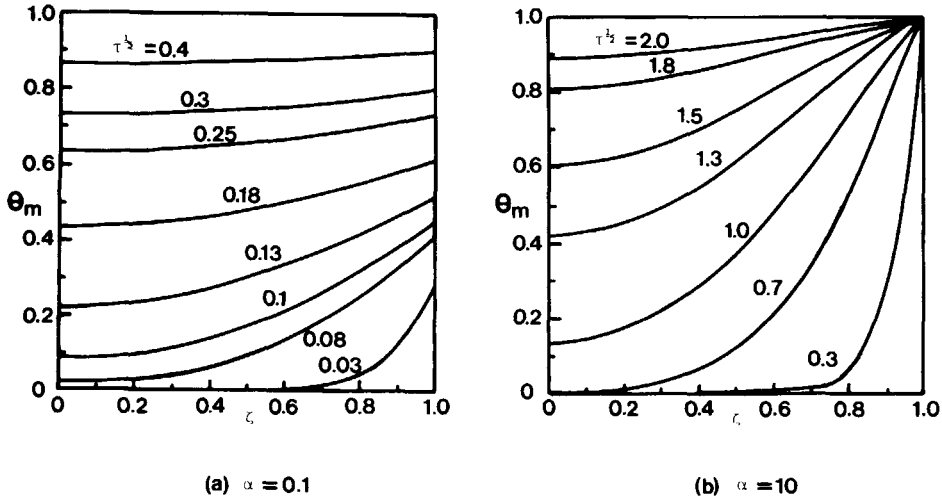

Fig. 4. Effect of α on the concentration profile when $\beta = 1$ and $\delta = 0.2$; (a) $\alpha = 0.1$ and (b) $\alpha = 10$.

For small values of α, the diffusion rate through the pore space is relatively much faster than the permeation rate into the microparticle and then the concentration of the pore space is the same as that of bulk phase throughout the polymer bead. The fraction γ of the total monomer units is functionalized rapidly, followed by diffusion-controlled functionalization in the entire resin bead. Thus, the effect of β is relatively less important for small values of α. For large values of α, however, the diffusion resistance through the pore space increases. Thus, as the value of β increases, that is, microparticle uptake increases, the rate of approaching to equilibrium slows.

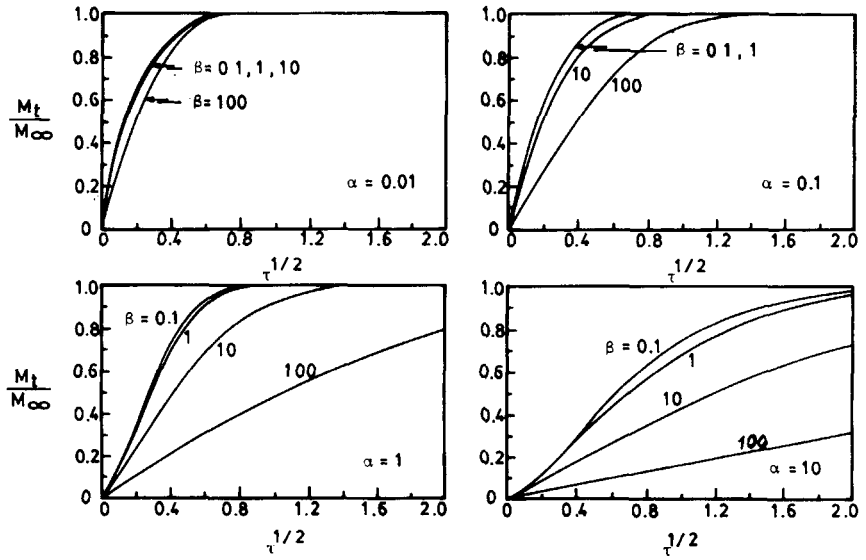

Fig. 5. Effect of the parameters, α and β, on the functionalization with $\delta = 0.2$; $\alpha = 0.01$, 0.1, 1, and 10.

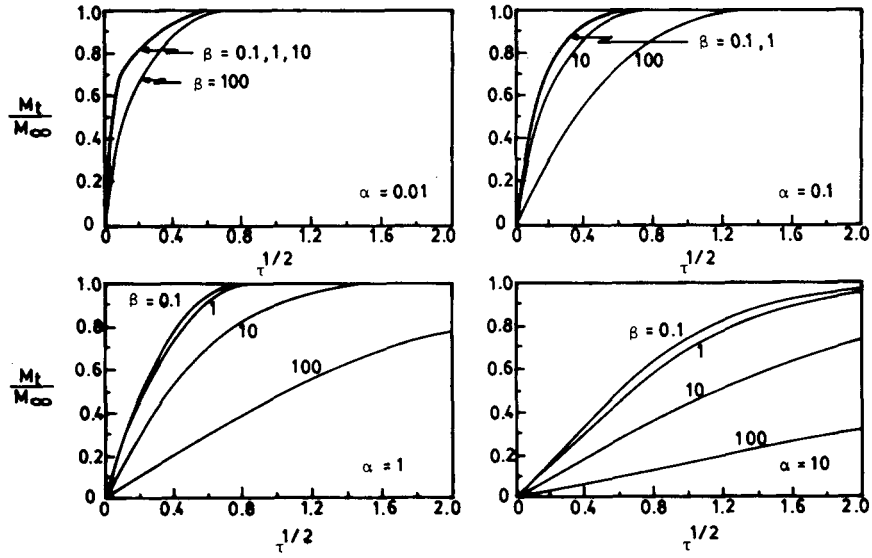

Fig. 6. Effect of the parameters, α and β, on the functionalization with $\delta = 0.6$; $\alpha = 0.01$, 0.1, 1, and 10.

RESULTS AND DISCUSSION

The typical electron micrographs are shown in Figure 7 for the chlorination at 90°C and at 20, 145, and 326 min. The gelular bead shows a very steep chlorine profile while the macroreticular bead indicates a rather deep chlorination over the bead sphere. From each picture, the diameter of the bead and the chlorine conversion (i.e., M_t/M_∞) can be obtained.

Effective Permeability of the Chlorine in the Gelular Bead

The conversion, M_t/M_∞, is related to the dimensionless time $\tau(= D_g t/[R_g(1 + K_g)])$ through the Eq. (7). With R_g and t known, the value of $D_g/(1 + K_g)$ can be estimated. If $D_g/(1 + K_g)$ is taken as an effective permeability, D_g', they are shown at different temperatures in Table I.

Effective Diffusivity of Chlorine in the Macroreticular Bead

The concentration profiles of chlorine by EDX show their gradients over the radii of both macroreticular and gelular resin beads. This indicates that the chlorination in the present study is controlled by both pore diffusion and gelular permeation.

The modeling parameters for SPC 108 were not known, but it was assumed that the values of β and δ are 20 and 0.03, respectively. The radius of microparticle, R_{mi} was further assumed to be 10^{-5} cm. Because there is no way of knowing the value of α, the conversions were plotted against the dimensionless time in Figure 8 by varying α from 0.01, 0.1, 1.0, to 10. For each value of α, both the macropore diffusivity and the gelular microparticle permeability can be calculated, and they are listed in Table II. It is shown that at 30°C the value of $D_{mi}'(= D_{mi}/[1 + (1 - \gamma)K_{mi}])$ ranges from 10^{-17} to 10^{-16} cm^2/s while that of $D_{ma}'(= \epsilon D_{ma}/(\epsilon + \gamma K_{ma})$ is from 10^{-10} to 10^{-8}

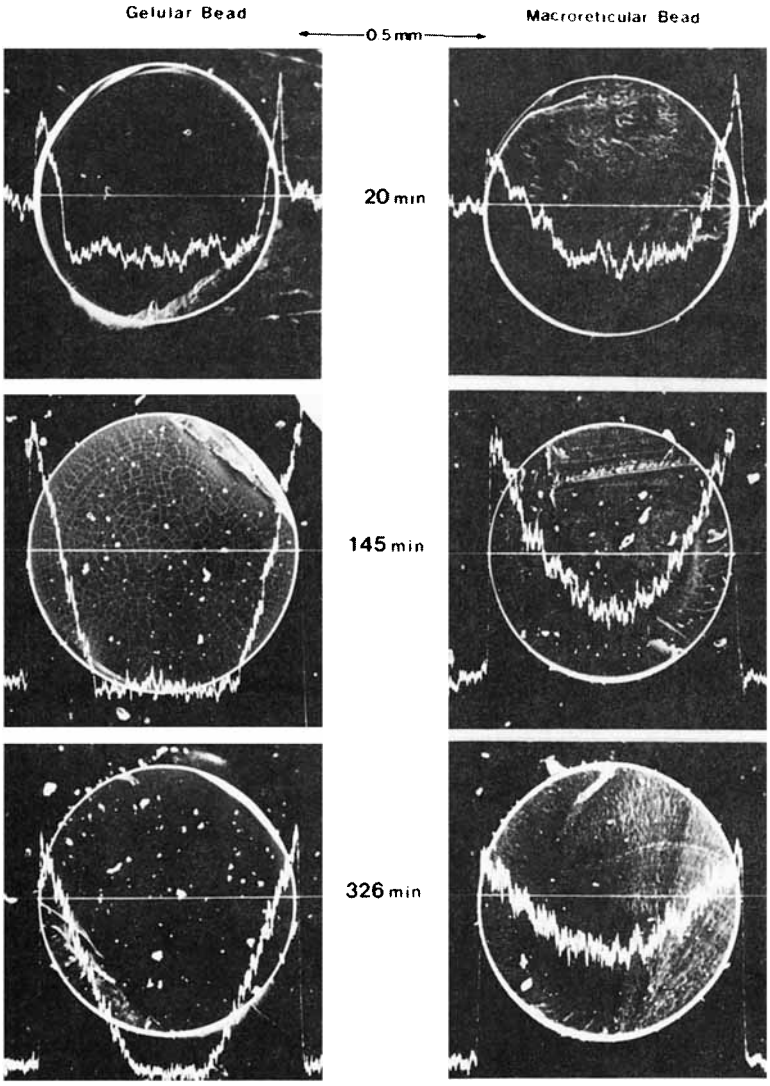

Fig. 7. Electron micrographs of the chlorine profile for the chlorination at 90°C.

TABLE I
Effective Permeabilities in the Gelular Bead

Temperature (°C)	Effective permeability (cm^2/s)
30	2.3×10^{-11}
50	9.7×10^{-11}
70	4.3×10^{-10}
80	9.4×10^{-10}
90	2.0×10^{-9}

TABLE II
Macropore Diffusivities and Gelular Microparticle Permeabilities in the Macroreticular Resin Bead

α	0.01		0.1		1		10	
T (°C)	D'_{mi}	D'_{ma}	D'_{mi}	D'_{ma}	D'_{mi}	D'_{ma}	D'_{mi}	D'_{ma}
30	6.7×10^{-17}	4.7×10^{-8}	1.0×10^{-16}	7.0×10^{-9}	2.6×10^{-16}	2.0×10^{-9}	5.8×10^{-16}	4.0×10^{-10}
50	1.5×10^{-16}	8.3×10^{-8}	2.5×10^{-16}	1.3×10^{-8}	5.0×10^{-16}	2.7×10^{-9}	1.3×10^{-15}	7.3×10^{-10}
70	3.8×10^{-16}	2.6×10^{-7}	5.2×10^{-16}	3.6×10^{-8}	1.1×10^{-15}	7.5×10^{-9}	3.2×10^{-15}	1.6×10^{-9}
80	5.1×10^{-16}	6.2×10^{-7}	6.6×10^{-16}	8.1×10^{-8}	1.7×10^{-15}	2.1×10^{-8}	4.5×10^{-15}	6.0×10^{-9}
90	7.3×10^{-16}	7.2×10^{-7}	8.8×10^{-16}	8.9×10^{-8}	2.3×10^{-15}	2.3×10^{-8}	5.2×10^{-15}	1.3×10^{-8}

cm^2/s. At 90°C, D'_{mi} ranges from 10^{-16} to 10^{-15} cm^2/s and D'_{ma} from 10^{-8} to 10^{-7} cm^2/s.

The result in the present study indicates that the effective microparticle permeability D'_{mi} (10^{-17}–10^{-15} cm^2/s) is smaller by several orders of magnitude than the gelular effective permeability D'_g (10^{-11}–10^{-9} cm^2/s). Since the gelular and macroreticular resin beads were chlorinated under the same condition, it is reasonable to assume that K_g and K_{mi} will be likely the same. Therefore, D_{mi} is also smaller by several orders of magnitude than D_g. This is rather surprising because poly(styrene-co-divinylbenzene) resin with 8% crosslinking might be considered to have the same gelular diffusivity for the gelular and macroreticular resin bead. This seems to be due to the inhomogeneous matrix structure of the microparticle formed by an inert solvent in the macroreticular bead. It is considered that for a gelular bead a more uniform crosslinking is assumed whereas the microparticles of the macroreticular bead may be more inhomogeneous in structure.

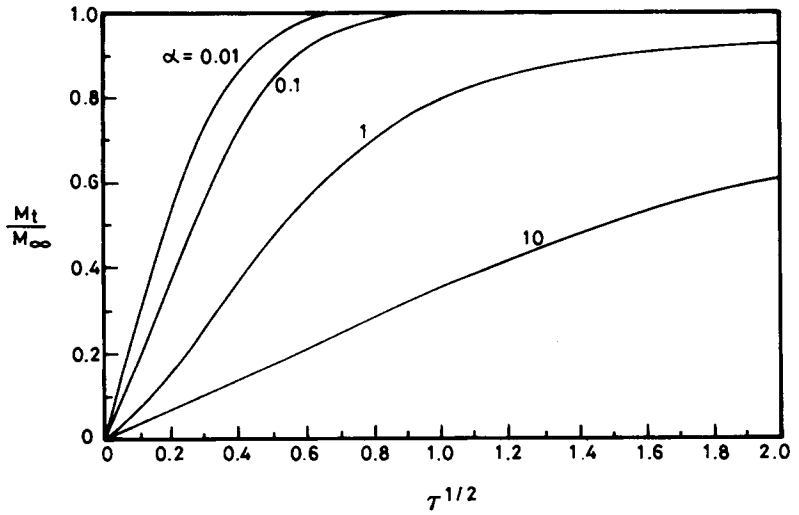

Fig. 8. Effect of α on the chlorination of macroreticular resin bead (SPC 108) when $\beta = 20$ and $\delta = 0.03$.

CONCLUSIONS

The diffusional process in the chlorination of sulfonated poly(styrene-co-divinylbenzene) has been studied through a general model as well as direct observation with electron microprobe. The two-phase model has been applied to analyze the chlorine profile and the conversion in macroreticular resin bead. The estimation of effective diffusivity from the EDX data suggests that the permeability of chlorine in the gelular bead is larger by several orders of magnitude than that for the gelular microparticle of the macroreticular bead.

Part of this work has been carried out during the stay of S. K. Ihm at TU Braunschweig as a research fellow of Alexander von Humboldt Foundation during 1983–1984.

NOMENCLATURE

C	concentration, mol/cm^3
D	diffusivity, cm^2/sec
D'	effective diffusivity, cm^2/sec
K	equilibrium constant, dimensionless
M	total amount of functionalized reactant, mol
r	distance from particle center, cm
R	particle radius, cm
S	concentration of functionalized reactant, mol/cm^3
t	time, sec

Greek

α	dimensionless rate parameter, $D'_{mi}R^2_{ma}/D'_{ma}R^2_{mi}$
β	dimensionless parameter, $3(1-\epsilon)[1+(1-\gamma)K_{mi}]/[\epsilon+\gamma K_{ma}]$
δ	dimensionless parameter, $\gamma K_{ma}/[\gamma K_{ma}+(1-\gamma)K_{mi}]$
γ	fraction of monomer present on the internal surface
ϵ	porosity
ξ	dimensionless gelular particle radial position
ζ	dimensionless macroreticular bead radial position
τ	dimensionless time

Superscript

o	bulk

Subscripts

a	pore space in macroreticular resin bead
g	gelular resin bead
i	gelular microparticle in macroreticular resin bead
t	transient
∞	equilibrium

References

1. P. Hodge and D. C. Sherrington, in *Polymer-Supported Reactions in Organic Synthesis*, John Wiley & Sons, New York, 1980.

2. A. R. Pitochelli, in *Ion Exchange Catalysis & Matrix Effects*, Rohm & Haas Co., Philadelphia, 1975.

3. K. A. Kun and R. Kunin, *J. Polym. Sci.* B., **2**, 587 (1964).
4. K. A. Kun and R. Kunin, *J. Polym. Sci.* C., **16**, 1457 (1967).
5. Z. Prokop and K. Setinek, *Coll. Czech. Chem. Commun.*, **42**, 3123 (1977).
6. J. Klein, H. Widdecke, and N. Bothe, *Makromol. Chem.* (Suppl.), **6**, 211 (1984).
7. C. R. Costin, Rohm and Haas XN1011, U.S. Patent 4269943 (1981).
8. Z. Prokop and K. Setinek, *Coll. Czech. Chem. Commun.*, **47**, 1613 (1982).
9. J. Crank, in *The Mathematics of Diffusion*, 2nd ed., Oxford University Press, Oxford, 1956.
10. S. K. Ihm, S. S. Suh, and I. H. Oh, *J. Chem. Eng. Japan*, **15**, 206 (1982).
11. E. Ruckenstein, A. S. Vaidynathan, and G. R. Youngquist, *Chem. Eng. Sci.*, **26**, 1306 (1971).

Received December 1, 1987
Accepted December 11, 1987